JOURNAL OF Materials CHEMISTRY

Effect of heteroatoms on photocurrent generation from a series of styryl dye Langmuir–Blodgett films

Jie Zheng, Chun-Hui Huang,* Tian-Xin Wei, Yan-Yi Huang and Liang-Bin Gan

State Key Laboratory of Rare Earth Materials Chemistry and Applications, Peking University–The University of Hong Kong Joint Laboratory in Rare Earth Materials and Bioinorganic Chemistry, Peking University, Beijing 100871, China

Received 20th September 1999, Accepted 8th December 1999

A series of amphiphilic styryl dyes, 2-[4-bis(hexadecyl)aminostyryl]benzothiazole methiodide (**BTM**), 2-[4-bis(hexadecyl)aminostyryl]benzoxazole methiodide (**BOM**), and 2-[4-bis(hexadecyl)aminostyryl]benzimidazole methiodide (**BIM**), were synthesized and successfully transferred onto the conducting transparent indium–tin oxide (ITO) electrode as H-aggregates by using a Langmuir–Blodgett (LB) technique. The photoelectrochemistry of the dye monolayers was investigated in a traditional three-electrode cell. The coincidence of their action spectra with the absorption spectra on the ITO electrodes indicated that the aggregates of the dyes on the ITO electrodes were responsible for the generation of the cathodic photocurrents. Some factors such as applied bias voltage, electron donors and acceptors on the photocurrent generation have also been investigated. Under favorable conditions (-200 mV, 1 mg ml^{-1} methylviologen diiodide (MV^{2+})), the photoelectric conversion quantum yield can reach 4.2%, 0.96%, and 1.19% for **BTM**, **BOM** and **BIM** respectively. Semiempirical calculations indicated that charge-separated states of the dyes upon illumination are a key requirement for the photocurrent generation. A common mechanism of photocurrent generation in this system was proposed based on the experiments. Experimental results indicated that heteroatoms in the acceptor parts of the dyes have a great effect on the photocurrent generation.

Introduction

Design of artificial photosynthesis systems is a very attractive field due to their potential applications such as photoelectric materials, biological catalysts.[1–4] Among these systems, pigments such as porphyrin and chlorophyll with electron donor and acceptor groups at different ends have a highly efficient photoelectric conversion and could be a valid approach to mimicry of natural photosynthesis.[5] The Fujihira group found that only if the electron donor, acceptor and chromophores were linked in a line, could the maximum quantum efficiency of photoelectric conversion be achieved in organic LB films.[6] In recent years, our group has found that many typical second-order optical organic materials with a π-conjugation bridge between the donor and acceptor groups (D–π–A), such as hemicyanines and azopyridinium compounds, also have good photoelectric conversion properties, and that the properties of donor or acceptor groups as well as the number of chromophores strongly affect the quantum efficiency of the photoelectric conversion.[7] For example, our recent work indicated that for the hemicyanine system, the quantum efficiency of photoelectric conversion could be enhanced about twice by simply replacing the pyridinium cation with quinolinium in the acceptor portion.[8]

To explore further the relationship between dye structure and photocurrent response of organic LB films, we designed three amphiphilic styryl dyes: 2-[4-bis(hexadecyl)aminostyryl]benzothiazole methiodide (**BTM**), 2-[4-bis(hexadecyl)aminostyryl]benzoxazole methiodide (**BOM**), 2-[4-bis(hexadecyl)aminostyryl]benzimidazole methiodide (**BIM**). In this paper, we investigated the photocurrent generation from the dye monolayer LB films on indium–tin oxide (ITO) substrate. The effect of the heteroatoms (sulfur, oxygen, or nitrogen atom) on the photocurrent generation and quantum yield has been discussed according to the experimental data and semiempirical quantum calculations. A possible mechanism for photocurrent generation under different conditions was proposed.

Experimental

Materials

2-Methylbenzothiazole, 2-methylbenzoxazole, 2-methylbenzimidazole, were purchased from Aldrich. Hydroquinone (H_2Q), KCl, methyl iodide and other reagents were all analytical reagent grade and were used as received. Water (R 18 MΩ) used was purified by passing deionized water through an Easy Pure RT Compact ultrapure water system (Bornstead Co.). Methylviologen diiodide (MV^{2+}): 4,4′-bipyridyl was reacted

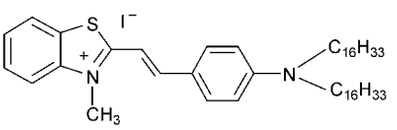

BTM

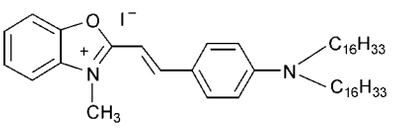

BOM

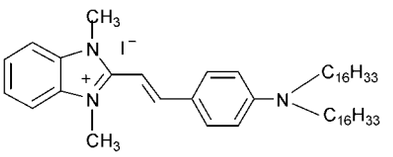

BIM

DOI: 10.1039/a907576c

with excess methyl iodide in refluxing ethanol for six hours. The product was filtered and washed with ethanol at least four times. Its identity was confirmed by using ^{1}H NMR spectroscopy.

Synthesis of the target compounds

The target compounds: 2-[4-bis(hexadecyl)aminostyryl]-benzothiazole methiodide (**BTM**), 2-[4-bis(hexadecyl)-aminostyryl]benzoxazole methiodide (**BOM**), and 2-[4-bis(hexadecyl)aminostyryl]benzimidazole methiodide (**BIM**) were obtained by condensing their methyl azolium precursors with 4-[bis(hexadecyl)amino]benzaldehyde (1 : 1 in molar ratio),[9] and the products were purified by column chromatography on silica gel with mixed chloroform–petroleum ether (bp 30–60 °C) (1 : 1) eluent. Their structures were confirmed by using elemental analysis and ^{1}H NMR.

BTM. Mp: 171 °C. Elemental analysis: Found: C: 68.10, H: 9.94, N: 3.17%. Calculated for $C_{48}H_{79}SN_2I$: C 68.40, H: 9.38, N: 3.32%. ^{1}H NMR ($CDCl_3$): δ 0.877 (t, 6H, $2CH_3$), 1.26 (m, 52H, $26CH_2$), 1.58 (t, 4H, $2CH_2$), 3.27 (t, 4H, $2CH_2$–N), 4.33 (s, 3H, R_3–N^+–CH_3), 6.49 (d, 1H, –CH=CH), 6.54 (d, 1H, –CH=CH), 7.45 (d, 2H, Ar–H), 7.51 (m, 1H, Ar–H), 7.66 (d, 1H, Ar–H), 7.78 (d, 1H, Ar–H), 7.86 (m, 1H, Ar–H), 8.04 (d, 2H, Ar–H).

BOM. Mp: 168 °C. Elemental analysis: Found: C: 69.5, H: 9.43, N: 3.12%. Calculated for $C_{48}H_{79}ON_2I$: C 69.7, H: 9.56, N: 3.38%. ^{1}H NMR ($CDCl_3$): δ 0.87 (t, 6H, $2CH_3$), 1.24 (m, 52H, $26CH_2$), 1.70 (t, 4H, $2CH_2$), 3.22 (t, 4H, $2CH_2$–N), 4.48 (s, 3H, R_3–N^+–CH_3), 6.94 (d, 1H, –CH=CH), 7.06 (d, 1H, –CH=CH), 7.52 (d, 2H, Ar–H), 7.69 (m, 1H, Ar–H), 7.80 (d, 1H, Ar–H), 8.18 (d, 1H, Ar–H), 8.31 (m, 1H, Ar–H), 8.83 (d, 2H, Ar–H).

BIM. Mp: 163 °C. Elemental analysis: Found: C: 68.5, H: 10.1, N: 4.68%. Calculated for $C_{49}H_{82}N_3I$: C 70.0, H: 9.84, N: 5.00%. ^{1}H NMR ($CDCl_3$): δ 0.878 (t, 6H, $2CH_3$), 1.259 (m, 52H, $26CH_2$), 1.558 (t, 4H, $2CH_2$), 3.24 (t, 4H, $2CH_2$–N), 3.90 (s, 3H, R_3–N–CH_3), 4.19 (s, 3H, R_3–N^+–CH_3), 6.45 (d, 1H, –CH=CH), 6.77 (d, 1H, –CH=CH), 7.35 (d, 2H, Ar–H), 7.54 (m, 1H, Ar–R), 7.63 (d, 1H, Ar–H), 7.64 (d, 1H, Ar–H), 7.78 (m, 1H, Ar–H), 7.81 (d, 2H, Ar–H).

Apparatus

Elemental analyses were carried out on Carlo Erba 1106 and Heraeus CHN-Rapid instruments. ^{1}H NMR spectra were measured using a Bruker ARX400 NMR spectrometer with tetramethylsilane as an internal standard (in $CDCl_3$). UV–Vis spectra were recorded using a Shimadzu UV-3100 spectrometer. Films were formed and deposited on the ITO electrode by using a Langmuir trough (Nima Technology Model 622).

LB film formation

Samples of the dyes in chloroform solution (0.24–0.3 mg ml^{-1}) were spread onto a water subphase at 20$\pm$1 °C. After the evaporation of the solvent, the films were compressed at the rate of 80 cm^2 min^{-1}, and then the monolayers of dyes were transferred respectively, under a surface pressure of 30 mN m^{-1}, onto transparent electrodes of indium–tin oxide (ITO)-coated borosilicate glass (the resistance was 250 Ω). To ensure the formation of the hydrophilic surface, the plate was immersed for 2 days in a saturated sodium methanol solution and then thoroughly rinsed with pure water under ultrasonication several times. Monolayer was formed on the ITO electrode. Films with transfer ratio *ca.* 1.0$\pm$0.1 were used in the experiments.

Photoelectrochemical and electrochemical measurements

A 500 W Xe arc lamp was used as the light source in the photoelectrochemical studies and various filters (*ca.* 300–800 nm) were used to obtain different wavelengths. The intensity of light was measured with an energy and power meter (Scientech, USA). A conventional glass three-electrode cell with the film-fabricated ITO electrode as the working electrode, a polished Pt wire as the counter-electrode, and saturated calomel electrode (SCE) as the reference electrode were used in the measurements. The supporting electrolyte was an aqueous solution of 0.5 M KCl in the photoelectrochemical studies and 0.1 M KCl in the electrochemistry experiments. All experimental data were recorded using a model CH 600-voltammetric analyzer controlled by a computer. In the electrochemical measurements, the solution was deoxygenated with bubbling nitrogen for at least 15 min. The effective illuminated area of the working electrode was 0.5 cm^2 in all photoelectrochemistry experiments.

Semiempirical quantum calculation

In the present work, AM1 in the program system MOPAC 7.0 was used to optimize the geometric structure of the dye congeners. MINDO/3 in the program systems MOPAC 7.0 was used to calculate the net charge of the atoms. The charge distribution in one part is obtained from the sum of the net charge of the atoms in this part.

Results and discussion

Characterization of LB films

The amphiphilic styryl dyes were characterized by the measurement of their surface pressure-area isotherms in the monolayer on the water subphase at pH 5.6. As is shown in Fig. 1, their collapse pressures are near 50 mN m^{-1}, and limiting areas are 53, 47, and 72 Å^2 for **BTM**, **BOM**, and **BIM** respectively. The larger limiting area of **BIM** probably results from its external methyl group at its heteroaromatic ring. The different limiting areas for the dyes suggest that the large bulky head groups determine the packing density in the monolayers. Fig. 1 reveals that the three dyes have good film formation properties.

Fig. 2 shows the absorption spectra of the dyes on the ITO electrode. The maximum absorption wavelengths of the dyes are blue shifted from 564, 534 and 429 nm in chloroform solution to 459, 473 and 426 nm on monolayer-modified ITO electrode for **BTM**, **BOM** and **BIM** respectively. Such blue shifts suggest the formation of long-range ordering H-aggregates (“head to head”) for all the dyes on the ITO electrodes. The results are in agreement with observations for hemicyanine LB films.[10]

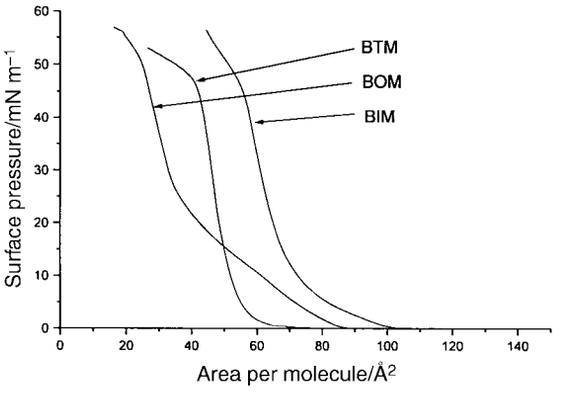

Fig. 1 Surface pressure–area isotherms of **BTM**, **BOM** and **BIM** at the air/water interface (20$\pm$1 °C).

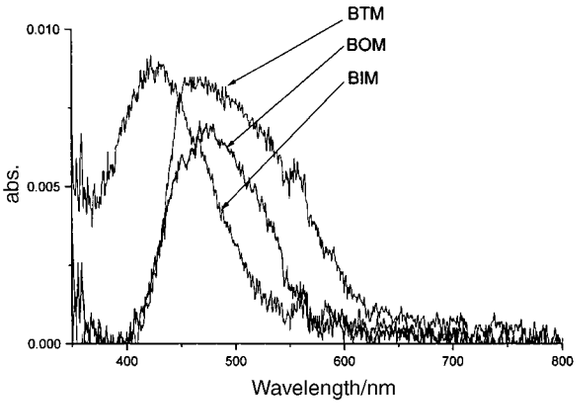

Fig. 2 Absorption spectra of **BTM**, **BIM** and **BOM** on the ITO substrate.

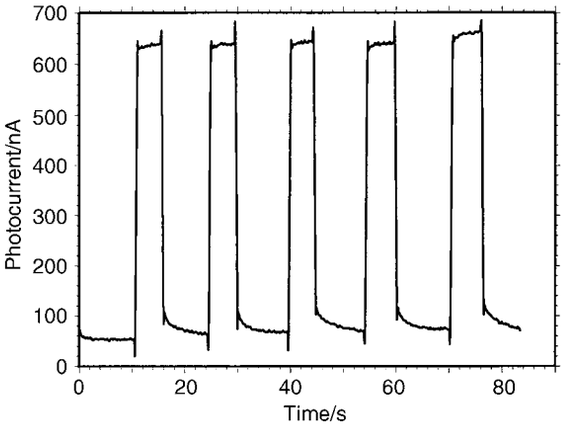

Fig. 3 Photocurrent generation from **BIM**–ITO electrode upon irradiation with white light at 258 mW cm^{-2} in 0.5 M KCl solution (0.5 cm^2 illuminating area).

Photocurrent generation from the dye–ITO electrodes

Steady cathodic photocurrents, ranging from 400 to 1400 nA cm^{-2} for the three dyes, flowed instantly when these dye-monolayer fabricated ITO electrodes were illuminated by white light of 258 mW cm^{-2} respectively, and fell as soon as irradiation was terminated. The photoelectric responses for the three dyes were very stable even after switching on and off many times. Fig. 3 shows an example of the experiments. The photocurrent action spectra were obtained by illuminating the dye-fabricated ITO electrodes respectively under variable wavelength monochromated light (shown in Fig. 4). The action spectra for the dyes are coincident with their absorption spectra on ITO electrodes (Fig. 2) respectively. About 10 nA anodic photocurrent was generated when a blank ITO electrode was irradiated. These results confirmed that photoinduced electron transfer took place and the aggregates of the dyes on the ITO electrodes were responsible for the generation of photocurrents. The cathodic photocurrents suggest that electrons flow from the electrode through the LB films to the electrolyte. Table 1 shows the photoelectric properties for the dyes. It can be clearly seen that under illumination with monochromated 464 nm light with 7.3×10^{15} photon cm^{-2} s^{-1}, photocurrents of 157.4, 28.2 and 87.6 nA cm^{-2}, for **BTM**, **BOM** and **BIM**, respectively were obtained. The corresponding quantum efficiencies are 0.73%, 0.17% and 0.47% for **BTM**, **BOM** and **BIM**, respectively. It can be seen that although these dyes' structures are similar, the quantum efficiency can be enhanced about 2.7 times or 4.2 times respectively by just replacing the oxygen atom in **BOM** with a nitrogen or sulfur atom to give **BIM** or **BTM** respectively. These experimental results suggest that heteroatoms have a great effect on the photocurrent generation for organic dyes.

As is known, photocurrent generation for organic dyes involves at least three processes: (1) formation of the photogenerated electron–hole pairs within a dye aggregate; (2) electron or hole migration within a dye aggregate; (3) electron transfer between the excited dye aggregates and another electron acceptor or donor in the systems.[2,11] To explore these processes in detail, the electrochemistry of dye monolayers on ITO electrode and the different factors on these processes were investigated as follows.

Electrochemical properties

In order to investigate the mechanism of photocurrent generation under different conditions in detail, the relevant energy levels in this system must be estimated. Cyclic voltammetric studies (sweep rate = 100 mV s^{-1}) were carried out in 0.1 M KCl neutral solution to estimate the redox potentials of the three dye monolayers on the ITO electrode. The oxidation potentials of the couples dye/dye^+ were obtained (1.01 V (**BTM**/$\mathbf{BTM}^+$), 1.01 V (**BOM**/$\mathbf{BOM}^+$), and 0.93 V (**BIM**/$\mathbf{BIM}^+$) with reference to SCE electrode respectively, shown in Table 2).

Effect of bias voltage

To study electron-transfer between the ITO electrode and LB films, the effect of bias voltage was investigated. Fig. 5 shows that there are good linear relationships between the potentials and photocurrents for the dyes within the range from −200 to 200 mV. The cathodic photocurrents increase as the potential of the working electrode becomes more negative relative to the SCE electrode *and vice versa*, indicating that photocurrents flow in the same direction as the applied negative voltage. Such negative voltage on the ITO electrode can form a strong electric field within the LB film (*ca.* 3 nm), which can accelerate the rate of charge migration within dye aggregates and the rate of electron transfer from the ITO electrode to the film, leading to enhancement of cathodic photocurrents. Open circuit voltages are obtained by extrapolating the lines until photocurrent is 0 nA. Their values are 0.2 V, 0.24 V and 0.27 V, for **BOM**, **BTM** and **BIM**, respectively.

Effect of electron acceptors and donor

To investigate the electron transfer between the excited aggregates and the electron donor or acceptors in the solution, the effects of electron donors and acceptors on photocurrent generation were studied. Fig. 6 shows that cathodic photocurrents increase on addition of MV^{2+} to the solution and then rise slowly with increasing concentration, indicating that MV^{2+} is a favorable factor for the generation of cathodic

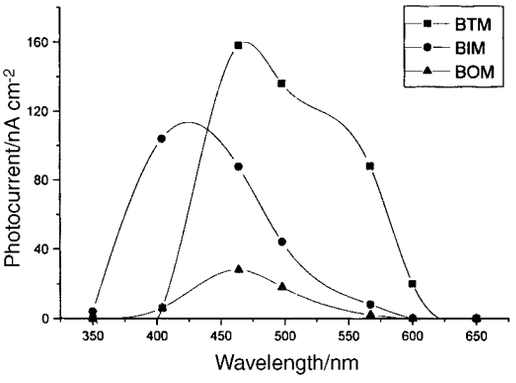

Fig. 4 Action spectra of the cathodic photocurrent for **BTM**, **BIM** and **BOM**. The intensities of photocurrent at the different wavelengths were all normalized.

Table 1 Photoelectric conversion property data of **BTM**, **BOM** and **BIM**

Compd.	I^a/nA cm^{-2}	I^b/nA cm^{-2}	φ^b (%)	I^c/nA cm^{-2}	φ^c (%)
BTM	1224	157.4	0.73	898	4.2
BOM	457	28.2	0.17	160	0.96
BIM	1110	87.6	0.49	222	1.19

I^a: the photocurrent under the irradiation of the white light (258 mW cm^{-2}) in 0.5 M KCl solution under the ambient conditions. I^b and φ^b: the photocurrent and the quantum efficiency under the irradiation of 464 nm monochromated light in 0.5 M KCl solution under ambient conditions. I^c and φ^c: the photocurrent and the quantum efficiency under the irradiation of 464 nm monochromated light in 0.5 M KCl solution with 1 mg ml^{-1} MV^{2+}, −200 mV bias voltage.

photocurrent. The enhancement of the photocurrents is because MV^{2+} is a strong electron acceptor, which can accept electrons from the film and accelerate the rate of electron transfer from the film to the solution, thus increasing the cathodic photocurrent.[11] However, it can be seen from Fig. 6 that dependence of the photocurrent on the MV^{2+} concentration for the dyes is distinctive. In particular, for **BIM**, the increase of the photocurrent with addition of MV^{2+} is far smaller than that of the others, which suggests that electron transfer between **BIM** and MV^{2+} is less efficient than that between **BOM** or **BTM** and MV^{2+}. The effect of oxygen on the electron transfer process was also investigated. Fig. 7 shows that when O_2 is removed from the solution by bubbling N_2, the cathodic photocurrents decrease gradually and reach stable values until the saturation of N_2 in the solution. The experimental results suggest that the presence of O_2 favors this process because it can act as an electron acceptor to form a superoxide anion radical,[12] and accelerate the electron transfer from the film to the solution. When H_2Q is added to the solution, the cathodic photocurrents for the three dyes decrease so quickly that they become anodic photocurrents, and then gradually level off when the H_2Q concentration is larger than 0.08 mg ml^{-1} in the solution (Fig. 8). The experimental results indicate that the existence of a strong electron donor is unfavorable to generation of the cathodic photocurrent. Although electron acceptors or donors have different effects on the electron-transfer process from the film to the solution, they do not affect the formation of photogenerated electron–hole pairs within a dye aggregate, which is related to photoinitiated intramolecular charge transfer of the dyes in the excited states.[13]

Semiempirical quantum calculations

To understand further the relationship between the heteroatom and photoinduced intramolecular charge transfer as well as photocurrent generation, it is necessary to clarify the charge distribution in the ground states and the excited states of the dyes. Based on neglecting the interaction of molecules on the film, semiempirical quantum calculation measurements are used to study the charge distribution in different states of the dye congeners: (2-(4-dimethylaminostyryl)benzothiazole methiodide **CBTM**, 2-(4-dimethylaminostyryl)benzoxazole methiodide **CBOM**, and 2-(4-dimethylaminostyryl)benzimidazole methiodide **CBIM**. First, the geometric structures of dye congeners are optimized by using the AM1 model Hamiltonian in the MOPAC 7.0 quantum chemical package.[14] Second, the charge distributions in the ground state and the excited state have been calculated by using MINDO/3 in the MOPAC 7.0 method. The symmetry deviation parameter Σ, defined as the sum of the charge density on one half of the ethylene chain minus the sum on the other half, is used to describe the extent of symmetry of the charge distribution.[15] The charge distributions at the different parts of the dye congeners in the different states are shown in Table 3. It can be clearly seen from Table 3 that the values of Σ_g for **BTM**, **BOM**, and **BIM** are 0.51, 0.45, and 0.36, indicating that the positive charges are mainly located on the acceptor parts for all the dyes in the ground state. In the excited state, the values of Σ_e become −0.01, 0.04 and −0.03 for **BTM**, **BOM** and **BIM** respectively. Large decreases in the Σ values in the excited state suggest an intramolecular charge transfer from the donor group to the acceptor group in the excited state and hence formation of a charge-separated state,[16] which is critical to photocurrent generation for this type of molecule with a D–π–A structure. The calculation results are also in agreement with the proposal of Gust *et al.* of formation of the charge-separated state for Donor–Sensitizer–Acceptor (D–S–A) photosynthetic systems,[5] and are also in accordance with the intramolecular charge separation upon illumination with a laser of nonlinear optical molecules with a D–π–A structure.[17] It can be seen from Table 3 that charge distributions for the dyes vary on changing the heteroatom in the system shown. For instance, for **BTM** and **BIM**, in contrast to their charge distribution in the ground state, the donor parts become more positive than the acceptor parts in the excited state, while for **BOM**, the positive charge in the acceptor part is still larger than that in the donor part in the excited state. These results indicate that the charge transfer between the donor and acceptor groups may be more effective in **BTM** and **BIM** than in **BOM**, which is probably a major reason for the lower quantum yield for **BOM** than the others.

Mechanism of photocurrent generation from the dye–ITO electrodes

It is known that photoinduced electron transfer involves the transfer of electrons between the different energy levels,[1,5] thus to elucidate the detailed mechanism of electron transfer under different conditions, the energy levels of the relevant electronic states are estimated. The conduction band E_c and valence band E_v of the ITO electrode are known to be *ca.* −4.5 eV and −8.3 eV, on an absolute scale, respectively. The reduction potential of MV^{2+} is about −4.51 eV, and the oxidation potential of H_2Q is −4.61 eV on the absolute scale.[11] With reference to the oxidation potential of 1.01 V, 1.01 V, and 0.93 V (*vs.* SCE) and band gap of 2.75 eV (459 nm), 2.62 eV (473 nm), and 2.91 eV (426 nm), the HOMO energy levels available for donating electrons are −5.75 eV, −5.75 eV and

Table 2 The HOMO and LUMO energy levels of **BTM**, **BOM** and **BIM**

Energy level	**BTM**[a]/eV	**BOM**[a]/eV	**BIM**[a]/eV	ITO[b]/eV
HOMO	−5.75	−5.75	−5.67	−8.3
LUMO	−3.05	−3.13	−2.76	−4.5
Band gap	2.75 (459 nm)	2.62 (473 nm)	2.91 (426 nm)	3.82 (325 nm)

[a]The energy levels of the dyes are obtained from the oxidation potentials from cyclic voltammetry of the dye monolayers in 0.1 M KCl solution (sweep rate = 100 mV s^{-1}). [b]Values obtained from reference 11.

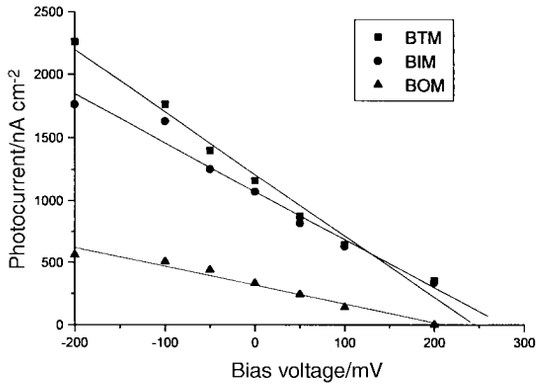

Fig. 5 Photocurrent *vs.* electrode potential for LB films of **BTM**, **BIM** and **BOM** under ambient conditions (258 mW cm^{-2} white light, 0.5 M KCl solution).

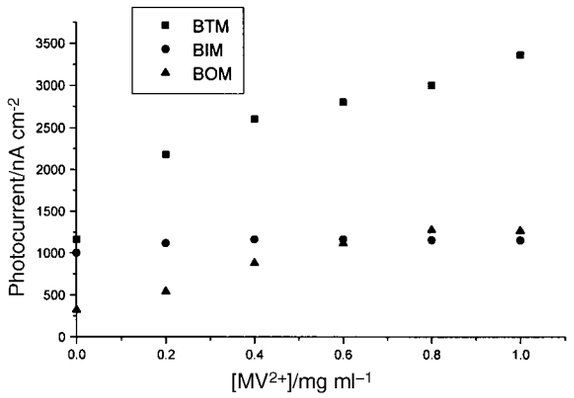

Fig. 6 The relationship between MV^{2+} concentration and photocurrents under ambient conditions (258 mW cm^{-2} white light, 0.5 M KCl solution) for **BTM**, **BIM** and **BOM**.

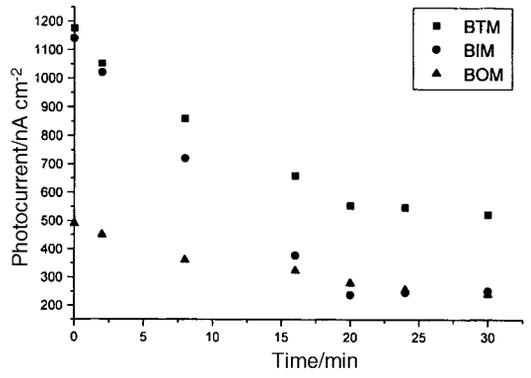

Fig. 7 Effects of N_2 on the photocurrents for **BTM**, **BIM** and **BOM** under ambient conditions (258 mW cm^{-2} white light, 0.5 M KCl solution).

−5.67 eV, and the LUMO energy levels available for accepting electrons are −3.05 eV, −3.13 eV and −2.76 eV, on an absolute scale, for **BTM**, **BOM** and **BIM** monolayer respectively (Table 2). Thus the detailed mechanism is shown in Scheme 1, indicating that when the dye aggregates are excited, the direction of photocurrents is not only dependent on the excited dye aggregates, but also on the nature of the redox couples around the electrode in the solution. For example, a cathodic photocurrent is generated through the following process: the dye aggregates are excited by absorbing light energy, and electrons transfer from the excited aggregates to the electron acceptor such as O_2 or MV^{2+} in the solution, and subsequently electrons from the conduction band of the ITO electrode are injected into the hole residing in the dyes

Table 3 The data of charge distribution at the different parts of the molecules in the ground state and the excited state for BTM, BOM and BIM

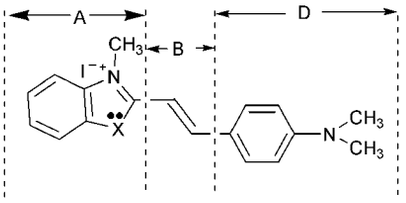

The ground state

X= S CBTM
X= N-CH_3 CBIM
X= O CBOM

	Ground state				First excited state			
Compd.	A_g[a]	B_g[b]	D_g[c]	Σ_g[d]	A_e[a]	B_e[b]	D_e[c]	Σ_e[d]
CBTM	0.73	0.05	0.22	0.51	0.51	−0.03	0.52	−0.01
CBOM	0.69	0.07	0.24	0.45	0.54	−0.04	0.50	0.04
CBIM	0.65	0.06	0.29	0.36	0.49	−0.01	0.52	−0.03

[a]Sum of the net charges of atoms at the acceptor part. [b]Sum of the net charge of atoms at the C=C bridge. [c]Sum of the net charge of atoms at the donor part. [d]Symmetry deviation parameter $\Sigma = A - B$.

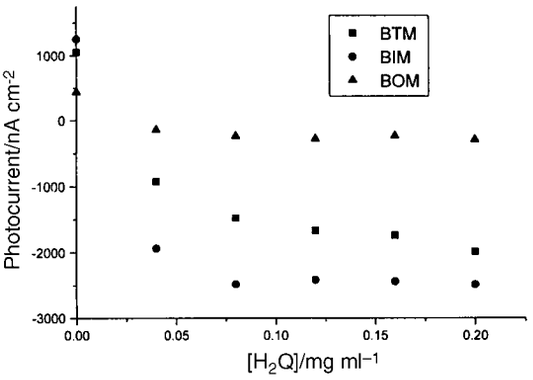

Fig. 8 Dependence of the photocurrent on the concentration of H_2Q under ambient conditions (258 mW cm^{-2} white light, 0.5 M KCl solution) for **BTM**, **BIM** and **BOM**.

aggregates. A strong electron donor such as H_2Q in the solution can donate electrons to quench the excited aggregates,[11] as a result of the formation of dye anion radicals, which can inject electrons into the conduction band of the ITO electrode, leading to the anodic photocurrent generation. It can be seen from Fig. 6 and Fig. 8 that the different dyes have different dependences of photocurrent on the concentration of MV^{2+} and H_2Q, which probably results from the differences between the energy levels of the electron donor or acceptor in the solution and different HOMO or LUMO energy levels for the dyes.[13]

The mechanism can also explain the observance of the order of open circuit voltages for the dyes (**BOM** < **BTM** < **BIM**). As is known, an open circuit voltage is related to the difference between the energy levels of dye aggregates and electron acceptor in the solution.[18] Under the same experimental conditions, the open circuit voltages are only determined by the energy level of the excited aggregates. According to the mechanism, the order of the energy level of the dye excited states is **BOM** < **BTM** < **BIM**, leading to the same sequence of open circuit voltages.

Under favorable conditions (1 mg ml^{-1} MV^{2+}, −200 mV), the quantum efficiencies can reach 4.2%, 0.96% and 1.19%, for **BTM**, **BOM**, and **BIM** respectively. It can be seen that under

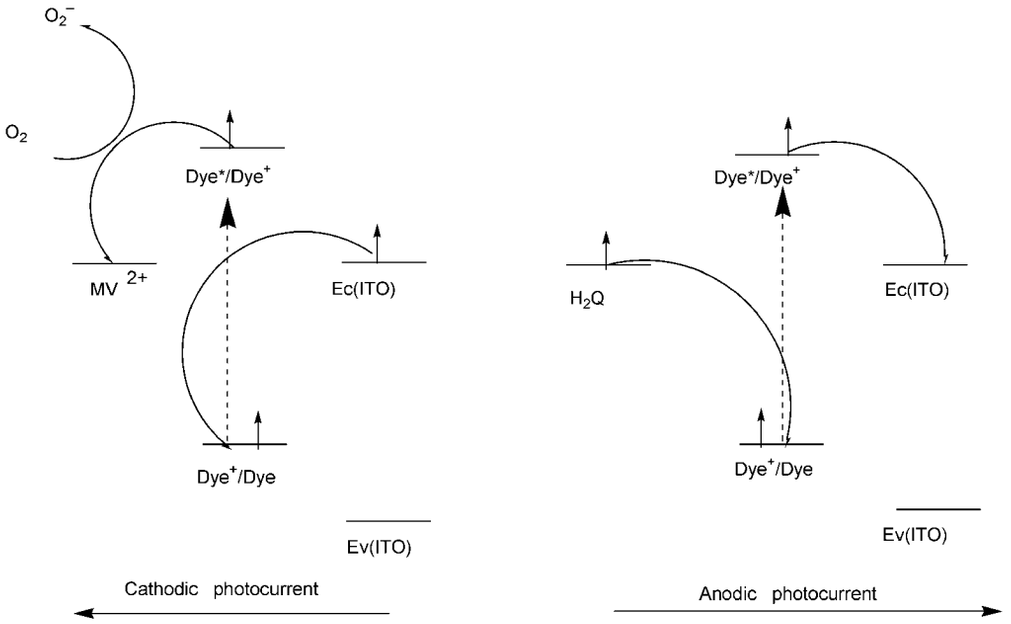

Scheme 1 Mechanism of photoinduced electron transfer for the dyes under different conditions.

favorable conditions, replacing the oxygen atom with sulfur can still enhance the photoelectric conversion quantum yield about 4.2 times relative to that under ambient conditions. While the quantum yield of **BIM** is only 1.2 times as large as that of **BOM** under favorable conditions, this value is smaller (2.7 times) than that under the ambient conditions, which suggests that an effective electron-transfer process from the films to solution is also a very important factor for photocurrent generation besides the formation of a charge-separated state. The values of quantum yields in these dye systems are among the largest values for organic dye systems on monolayer LB films (0.01–1.2%),[7,9,11,19] suggesting that these dyes have good photoelectric conversion properties and could be good candidates for organic photoelectric materials.

Conclusions

A series of styryl dyes were synthesized and photocurrent responses from the LB film fabricated ITO electrodes were investigated. Experimental data indicated that heteroatoms in the acceptor parts had a great effect on the photocurrent generation. Some other factors such as bias voltage, electron donor and acceptors have effects on the photocurrent generation. A possible photoinduced electron transfer mechanism was proposed. Studying the effect of heteroatoms on the photocurrent generation can provide us with a strategy for designing new organic photoelectric materials.

Acknowledgements

The authors thank the State Key Program of Basic Research (G1998061300) and National Natural Science Foundation of China for financial support on this project.

References

1 *Topics in Current Chemistry*, ed. J. Mattay, vol. 159, Springer-Verlag, 1991.
2 A. J. Bard, *Science*, 1980, **207**, 139.
3 A. M. Ratner and C. A. Mirkin, *Annu. Rev. Phys. Chem.*, 1992, **43**, 719.
4 G. Steinberg-Yfrach, J.-L. Rigaud, E. N. Durantini, A. L. Moore, D. Gust and T. A. Moore, *Nature*, 1998, **392**, 479.
5 D. Gust, T. A Moore and A. L. Moore, *Acc. Chem. Res.*, 1993, **26**, 198.
6 (*a*) M. Fujihira, *Mol. Cryst. Liq. Cryst.*, 1990, **183**, 59; (*b*) M. Fujihira and H. Yamada, *Thin Solid Films*, 1988, **160**, 125; (*c*) M. Fujihira, *Nanostruct. Mater.*, 1992, 27.
7 (*a*) W. S. Xia, C. H. Huang, L. B. Gan and C. P. Luo, *J. Phys. Chem.*, 1996, **100**, 15525; (*b*) D.-G. Wu, C.-H. Huang, L.-B. Gan, W. Zhang, J. Zheng, H.-X. Luo and N.-Q. Li, *J. Phys. Chem. B*, 1999, **103**, 4377; (*c*) T. R. Cheng and C. H. Huang, *J. Mater. Chem.*, 1997, **7**, 631.
8 A. D. Liang, J. Zhai, C. H. Huang, L. B. Gan, Y. L. Zhao, D. J. Zhou and Z. D. Chen, *J. Phys. Chem. B*, 1998, **102**, 1424.
9 E. Barni, P. Savarino, R. Larovere and G. Viscardi, *J. Heterocycl. Chem.*, 1986, **23**, 209.
10 D. G. Whitten, *Acc. Chem. Res.*, 1993, **26**, 502.
11 Y. S. Kim, K. Liang, Y. Law and D. G. Whitten, *J. Phys. Chem.*, 1994, **98**, 984.
12 A. Haraguchi, Y. Yonezawa and R. Hanawa, *Photochem. Photobiol.*, 1990, **52**, 307.
13 K.-Y. Law, *Chem. Rev.*, 1993, **93**, 449, and references cited therein.
14 M. Utinans and O. Neilands, *Adv. Mater. Opt. Electron.*, 1999, **9**, 19.
15 S. Dahne, *Z. Chem.*, 1981, **21**, 58.
16 (*a*) M. S. A. Abd-El-Mottaleb, *Z. Phys. Chem.*, 1983, **264**, 5, S. 957; (*b*) Ph. Hebert, G. Baldacchino, Th. Gustavasson and J. C. Mialocq, *J. Photochem. Photobiol. A: Chem.*, 1994, **84**, 45.
17 D. S. Chemla and J. Zyss, *Nonlinear optical properties of organic molecules and crystals*, Vol. 1 and 2, Academic Press, New York, 1987.
18 B. O'Regan and M. Gratzel, *Nature*, 1991, **353**, 737.
19 S. R. Forrest, *Chem. Rev.*, 1997, **97**, 1973, and references cited therein.

Paper a907576c